

EFFECT OF COPPER ON THERMAL STABILITY OF NANOCRYSTALLINE CERIA

ORIGINAL SCIENTIFIC PAPER

Katarina Mužina,¹✉ Aleksandar Bajrović,¹ Martina Župančić,² Stanislav Kurajica¹

DOI: 10.5281/zenodo.4059911

RECEIVED
2020-01-06ACCEPTED
2020-05-11

¹ University of Zagreb, Faculty of Chemical Engineering and Technology, Marulićev trg 19, 10000 Zagreb, Croatia
² Leibniz-Institut für Kristallzüchtung, Max-Born-Straße 2, 12489 Berlin, Germany

✉ kmuzina@fkit.hr

ABSTRACT:

Cerium (IV) oxide (CeO₂) is extensively used as a catalyst because it has numerous advantages over conventional catalysts, like low cost, better poisoning resistance, high catalytic activity due to the facile Ce⁴⁺ / Ce³⁺ redox reaction and high oxygen storage capacity. CeO₂ nanoparticles have higher specific surface area and better redox properties, and thus an increased catalytic activity in comparison to bulk materials. However, at elevated temperatures ceria nanoparticles are very prone to coarsening. In order to increase the thermal stability of CeO₂ nanoparticles, but also improve its catalytic properties, metal ions are incorporated into the CeO₂ crystal structure. The aim of this study was to compare coarsening kinetics of nanocrystalline CeO₂ and nanocrystalline CeO₂ doped with 10 mol. % of copper in order to determine the effect of doping on thermal stability. Samples were prepared by hydrothermal synthesis and thermally treated at different temperatures and processing times. The samples were analyzed by X-ray diffraction analysis and the crystallite sizes were calculated using the Scherrer's equation. Based on the obtained crystallite sizes, kinetic parameters were determined and it was found that copper addition has a positive effect on the thermal stability of CeO₂.

KEYWORDS: cerium (IV) oxide; coarsening kinetics; hydrothermal synthesis; doping

INTRODUCTION

Cerium (IV) oxide (CeO₂), also called ceria, is one of the most important and generally applied lanthanide oxides. It possesses a fluorite crystal structure with space group Fm3m, which is stable from room temperature till the melting point (~2 400 °C). Cerium has two stable oxidation states, Ce³⁺ and Ce⁴⁺, and the special feature of cerium (IV) oxide is that the fluorite lattice can withstand significant reduction of cerium without alteration or collapse of the structure, especially at elevated temperatures [1]. During the partial reduction of Ce⁴⁺ to Ce³⁺, oxygen molecules are released in order to maintain the electroneutrality of the crystal lattice, which causes the formation of oxygen vacancies. These vacancies can freely move within the crystal lattice and can also re-adsorb oxygen molecules from the air. The good catalytic properties of cerium (IV) oxide are attributed to this easiness of transition between oxidation states, which allows the formation of oxygen vacancies and the good mobility and high oxygen storage capacity within the crystal lattice [2]. Ceria has many advantages over traditional catalysts, like low price and availability, lower degree of thermal sensitivity, higher resistance to poisoning, while also allowing high conversions to be achieved for certain types of chemical processes. Cerium (IV) oxide is therefore

widely used as a heterogeneous catalyst in three-way catalytic converters in car exhaust systems, for the conversion of water gas to produce hydrogen for various industrial processes and for the removal of atmospheric pollutants such as volatile organic compounds [3-5]. Modern catalyst design is aimed at preparation of nanoscale catalysts because they possess superior properties in comparison to bulk materials due to greater surface to bulk atoms ratio. The atoms on the surface have unsatisfied chemical bonds and therefore possess greater energy than bulk atoms. Increased energy influences the band gap, morphology, reactivity, and catalytic potential of a heterogeneous nanocatalyst [6]. The problem with nanoparticles occurs at elevated temperatures since they are prone to aggregation and coarsening which cause the increase of crystallite sizes and the reduction of specific surface area. To solve this problem and to further improve the catalytic properties of ceria, transition metals having smaller radius and lower valence than cerium can be introduced into the ceria crystal lattice [7]. In this work, pure and Cu-doped ceria samples were prepared using a simple, affordable and eco-friendly hydrothermal method. The samples were characterized and then thermally treated at various temperatures and processing times. Coarsening kinetics analysis was performed in order to evaluate the

effect of the dopant on the thermal stability of cerium (IV) oxide.

EXPERIMENTAL

Samples of pure and copper doped ceria were prepared by hydrothermal method using the following procedure: The appropriate amounts of precursors, namely 0.8 mmol of $\text{Ce}(\text{SO}_4)_2 \cdot 4\text{H}_2\text{O}$ for pure sample as well as 0.72 mmol of $\text{Ce}(\text{SO}_4)_2 \cdot 4\text{H}_2\text{O}$ and 0.08 mmol of $\text{CuSO}_4 \cdot 5\text{H}_2\text{O}$ for Cu doped sample, were put in a Teflon-lined stainless-steel autoclave with a capacity of 70 cm^3 , which was then filled with 56 cm^3 of 8 mol dm^{-3} NaOH solution, sealed and placed in a temperature controlled oven at $120 \text{ }^\circ\text{C}$ for 16 hours. After the end of the reaction time, the autoclave was cooled down, the NaOH solution was decanted and the precipitate washed three times with demineralized water with help of sonification and centrifugation. The precipitate was then dried at $60 \text{ }^\circ\text{C}$ for 24 hours.

The pure and the doped sample were thermally treated at different temperatures and processing times (Table 1), after which X-ray powder diffraction (XRD) analysis was performed. The instrument used was Shimadzu XRD 6000 diffractometer with $\text{CuK}\alpha$ radiation operating at 40 kV and 30 mA in a step scan mode ranging from 5 to $105 \text{ }^\circ 2\theta$, with steps of $0.02 \text{ }^\circ 2\theta$ and counting time of 0.6 s.

Table 1. Temperatures and processing times for the pure and Cu doped sample.

300 °C	350 °C	400 °C	450 °C	500 °C
15 min	15 min	15 min	15 min	-
30 min	30 min	30 min	30 min	-
1h	1h	1h	1h	-
2h	2h	2h	2h	2h
4h	4h	4h	4h	-

The as-prepared pure and Cu doped sample were additionally analyzed using high resolution transmission electron microscopy (HRTEM) on transmission microscope JEOL ARM 200 CF. The samples were applied directly to a nickel grid and analyzed at accelerating voltage of 80 kV. ImageJ program was used for the analysis of the obtained micrographs [8]. In order to analyze the chemical composition of the samples, energy dispersive X-ray spectroscopy (EDS) analysis was performed on Tescan Vega Easy Probe 3 scanning electron microscope operating at 10 kV. Samples were fixed on a sample holder using double-sided carbon conductive tape.

RESULTS AND DISCUSSION

The obtained pure and Cu doped sample were first analyzed by XRD in order to gain insight into their phase composition and purity. The X-ray patterns are shown in figure 1. As can be seen, both the pure and the doped sample only contain peaks characteristic for cerium (IV) oxide (ICDD PDF No. 34-0394), which indicates that copper is incorporated in the ceria crystal lattice. Diffraction patterns can be used for the determination of crystallite sizes using the Scherrer's method (Eq. 1).

$$d = \frac{K\lambda}{B \cos \theta} \quad (1)$$

where d is the crystallite size, K is the shape factor which is 0.94 for spherical particles of cubic symmetry, λ is the $\text{CuK}\alpha$ radiation wavelength, θ is the Bragg angle and B is the peak full width at half maximum corrected for instrumental broadening.

Broad peaks usually point out to small crystallite sizes, which were proven by calculation, as seen in Table 2. The doped sample has a slightly lower crystallite size, but taking into account the limitations of the method, the difference between the pure and the doped sample is not significant.

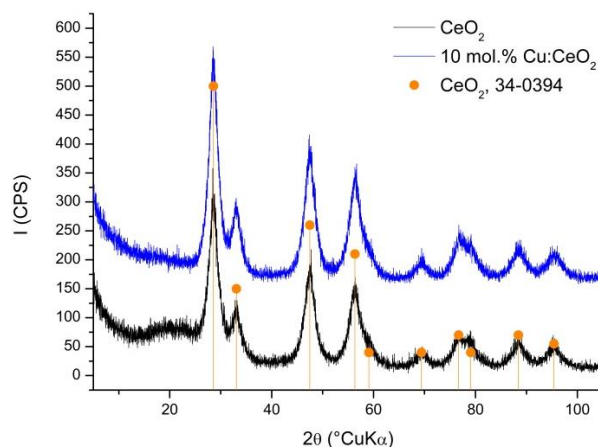


Figure 1. Diffraction patterns of the pure and the Cu doped sample.

HRTEM analysis (Figure 2) shows aggregates of fine nanocrystallites with sizes corresponding to the sizes obtained by the Scherrer's method (Table 3). The obtained nanoparticles have spherical morphology and there is no evident difference in morphology between the pure and the doped sample. The fringes distance of 2.7 \AA for both samples matches the (200) crystal plane of cerium (IV) oxide (ICDD PDF No.

34-0394). Since neither XRD nor HRTEM analysis show the presence of copper in the doped sample, it

can be indicated that a solid solution of copper in the ceria crystal lattice is formed.

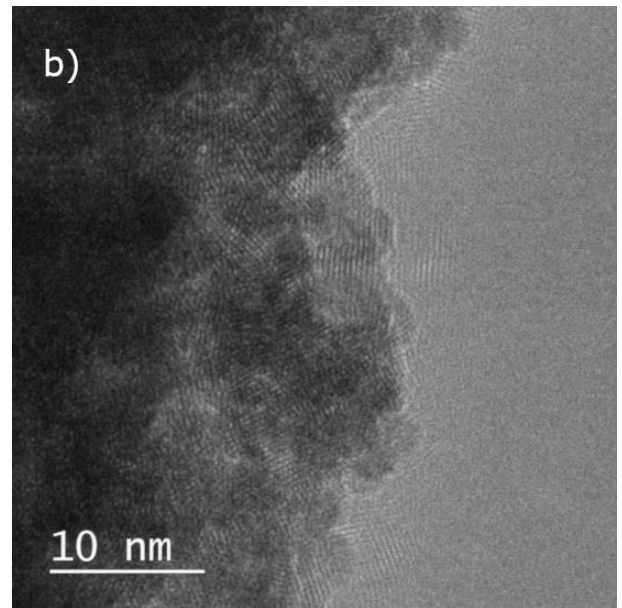
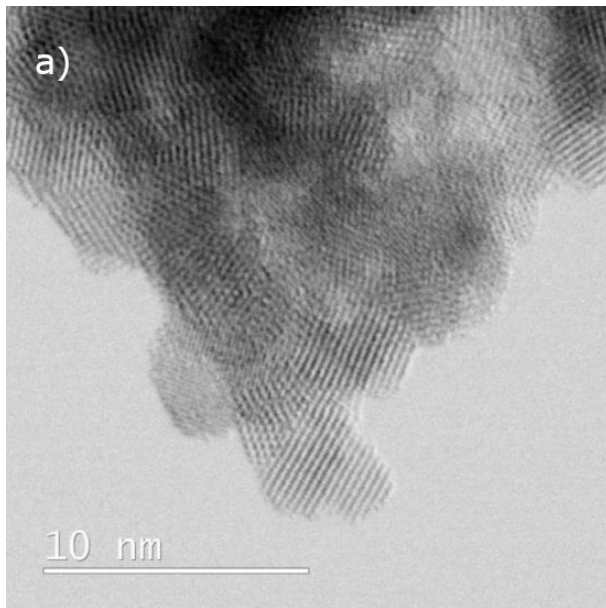


Figure 2. HRTEM micrograph of the pure (a) and Cu doped (b) sample.

Table 2. Crystallite sizes obtained from diffraction patterns by Scherrer's method and particle sizes and fringes distance obtained from micrographs using ImageJ program.

	CeO ₂	10 mol. % Cu:CeO ₂
Crystallite size (XRD)	4.2 nm	4.0 nm
Particle size (HRTEM)	~ 4 nm	~ 4 nm
Fringes distance	2.703 Å	2.730 Å

To confirm the presence of copper in the doped sample, EDS analysis was performed. Results are shown in figure 3. As can be seen, both the pure and the doped sample show the presence of cerium and oxygen, as well as carbon because of the carbon tape used for the fixation of the sample onto the sample holder. Peaks characteristic for copper are found in the doped sample proving the doping successful.

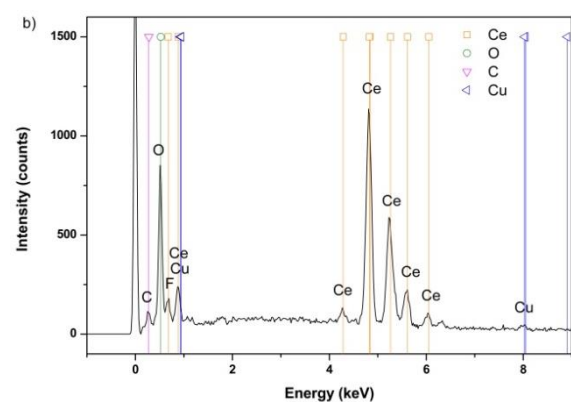
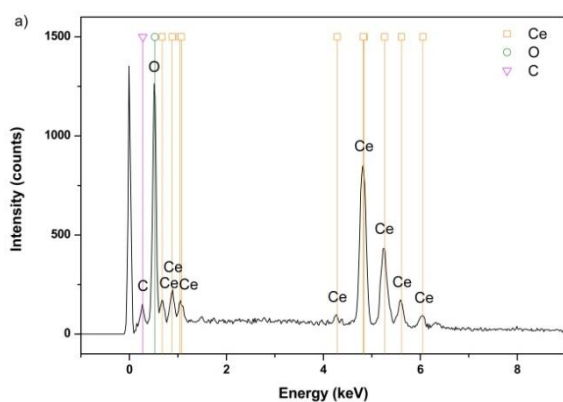


Figure 3. EDS spectra of the pure (a) and Cu doped (b) sample.

Both the pure and the doped sample were thermally treated at different temperatures and processing

times, as shown in Table 2, analyzed by XRD, and the crystallite size values were obtained using the

Scherrer's equation. The crystallite sizes were then used in the coarsening kinetics analysis based on the equations from the work of Lopez et al. [9], which are as follows:

$$d^n - d_0^n = Kt \tag{2}$$

Where d is the average particle size, d_0 is the initial particle size, n is the particle growth exponent, K is a constant dependent on temperature ($K = K_0 \exp(-Q/RT)$) and t is the time of thermal treatment.

This equation can be simplified to:

$$d = K't^m \tag{3}$$

Where m is equal to $1/n$, and it can be derived from the logarithmic plot of d versus t as the value of the slope:

$$\ln d = \ln K' + m \ln t \tag{4}$$

While the intercept $\ln K'$ is further used in the Arrhenius plot to obtain the activation energy, Ea :

$$\ln K' = \ln A - \frac{Ea}{RT} \tag{5}$$

Where A is the pre-exponential factor, Ea activation energy, R universal gas constant and T is the temperature expressed in Kelvins [9].

Our chosen temperatures of thermal treatment were lower than the ones in the work of Lopez et al., because the targeted application of our ceria nanoparticles is in catalytic oxidation of volatile organic compounds and exhaust gases from automobiles which need to be accomplished at lower temperatures (less than 500 °C). Figure 4 shows the dependence of crystallite size on temperature for 2 hours duration of thermal treatment, including the values of initial crystallite size for both the pure and the doped sample. It can be seen that for both samples the crystal growth depends exponentially on the temperature. However, crystallites in the Cu doped sample grow slower at lower temperatures in comparison to the pure sample, although the difference is not drastic. Crystal growth accelerates significantly at 500 °C.

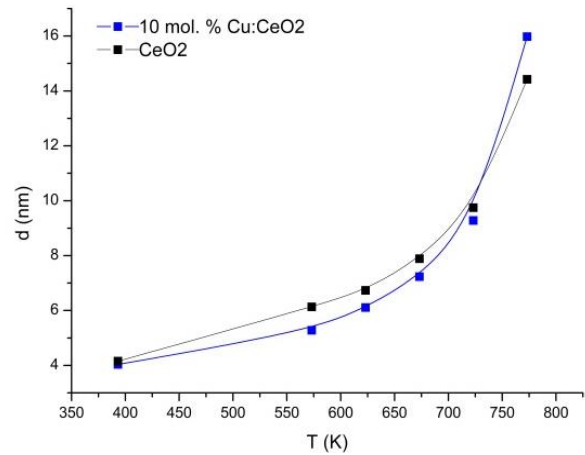


Figure 4. Initial size and crystallite sizes after thermal treatment for 2 hours for the pure and the doped sample.

The particle growth exponents (n) for the pure and the doped sample at various temperatures were determined from the logarithmic plots of d versus t (figure 5) and are listed in table 3.

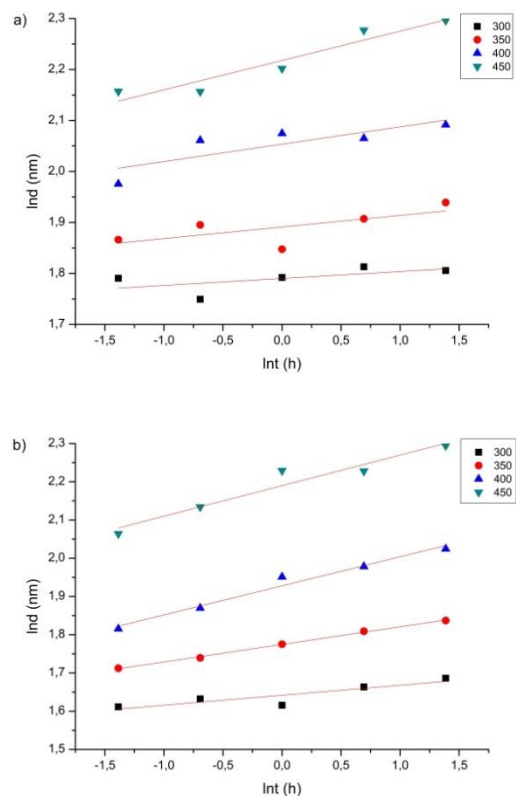


Figure 5. Plots of $\ln d$ vs $\ln t$ for the pure (a) and the doped (b) sample.

Equation 2 implies that high values of n point out to sluggish crystallite growth due to restricted boundary mobility [9], which is confirmed in this experiment since the n value is indeed higher at lower tem-

peratures. The values for the doped sample are lower which would indicate faster grain growth, but the calculated crystallite sizes are lower at lower temperatures than that of the pure sample, which would mean higher thermal stability.

Table 3. Particle growth exponent values for the pure and doped sample at various temperatures.

T (°C)	n (CeO ₂)	n (Cu:CeO ₂)
300	73	38
350	43	21
400	29	13
450	17	12

Activation energy values for the pure and the doped samples were obtained from the Arrhenius plots and are shown in figure 6.

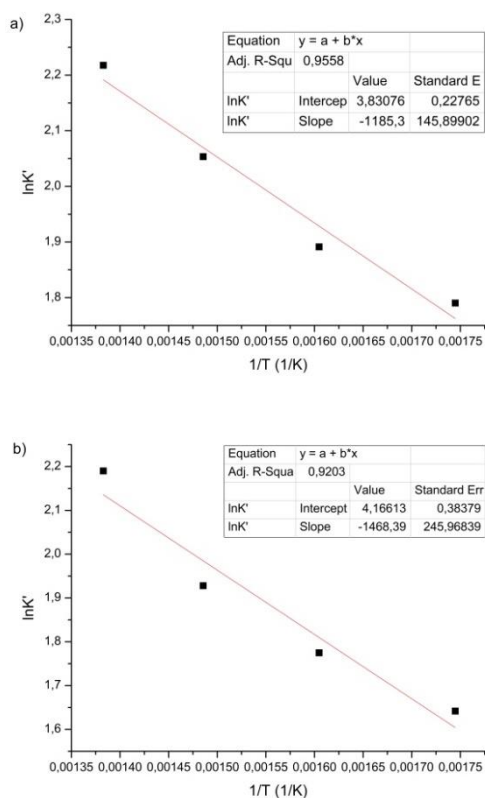


Figure 6. Arrhenius plot for the pure (a) and the doped (b) sample.

The obtained values are 9854 J/mol for the pure sample and 12208 J/mol for the Cu doped sample. The obtained values are much lower than in the literature [9, 10] because our research was done only for lower coarsening temperatures for the beforehand mentioned reasons. At lower temperatures no significant changes in ceria occur, except coarsening, which is not an extremely energy consuming process. The

activation energy is higher for the doped sample, which means that it is necessary to bring more energy to the system to induce nanoparticles coarsening and that the doped sample is indeed more thermally stable than the pure one.

CONCLUSION

Nanoparticles of pure and Cu doped ceria were prepared by hydrothermal method. Samples were thermally treated at different temperatures and different processing times, and a coarsening kinetics analysis was conducted. Crystallites in both samples grow with increasing temperature and time. The addition of copper increases the thermal stability of ceria indicated by the higher activation energy of the doped sample.

ACKNOWLEDGEMENT

This work has been fully supported by Croatian Science Foundation under the project IP-01-2018-2963. The sustenance of the University of Zagreb is gratefully acknowledged.

REFERENCES

- [1] L.F. Arenas, C. Ponce de León, F.C. Walsh, "Electrochemical redox processes involving soluble cerium species," *Electrochim. Acta.*, vol. 205, pp. 226-247, 2016.
- [2] M. Mogensen, N. M. Sammes, G. A. Tompsett, "Physical, chemical and electrochemical properties of pure and doped ceria," *Solid State Ion.*, vol. 129, pp. 63-94, 2000.
- [3] G. Ramakrishnan, K. Naveen, "Emission and dynamic characteristics of three way catalytic converter by computational fluid dynamics," *Int. J. Eng. Sci.*, vol. 6, pp. 3503-3510, 2016.
- [4] Z. Ren, F. Peng, J. Li, X. Liang, B. Chen, "Morphology-dependent properties of Cu/CeO₂ catalysts for the water-gas shift reaction," *Catalysts*, vol. 7 (2), pp. 48-60, 2017.
- [5] M. Duplančić, S. Kurajica, V. Tomašić, I. Minga, "Catalytic oxidation of toluene on hydrothermally prepared ceria nanocrystals," *Chem. Biochem. Eng. Q.*, vol. 31, pp. 375-383, 2017.
- [6] S. Kurajica, S. Lučić Blagojević, *Introduction to Nanotechnology* (In Croatian: *Uvod u nanotehnologiju*), HDKI, Zagreb, 2017.
- [7] L. Kundakovic, M. Flytzani-Stephanopoulos, "Cu- and Ag-Modified Cerium Oxide Catalysts for Methane Oxidation," *J. Catal.*, vol. 179, pp. 203-221, 1998.
- [8] C. A. Schneider, W. S. Rasband, K. W. Eliceiri, "NIH ImageJ: 25 years of image analysis," *Nat. Methods*, vol. 9, pp. 671-675, 2012.
- [9] H. F. Lopez, H. Mendoza, "Temperature Effects on the Crystallization and Coarsening of Nano-CeO₂ Powders," *ISRN Nanomaterials*, vol. 2013, Article ID 208614, 2013, <https://doi.org/10.1155/2013/208614>.
- [10] V. K. Ivanov, O.S. Polezhaeva, G. P. Kopitsa, P. P. Fedorov, K. Pranzas, V. V. Runov, "Specifics of High-Temperature Coarsening of Ceria Nanoparticles," *Russ. J. Inorg. Chem.*, vol. 54, no. 11, pp. 1767-1775, 2009.

THIS PAGE OF
TECHNOLOGICA ACTA
INTENTIONALLY LEFT BLANK